

MnO₂@Nickel Nanocone Arrays with High Areal Capacitance for Flexible Zinc-ion Supercapacitor

Long Qian

Division of Energy and Environment
Tsinghua Shenzhen International
Graduate school
Shenzhen, China
ql18@mails.tsinghua.edu.cn

Yongsheng Li

Division of Energy and Environment
Tsinghua Shenzhen International
Graduate school
Shenzhen, China
li-ys18@mails.tsinghua.edu.cn

Min Wang

Division of Energy and Environment
Tsinghua Shenzhen International
Graduate school
Shenzhen, China
wangmin17@mails.tsinghua.edu.cn

Cheng Yang*

Division of Energy and Environment
Tsinghua Shenzhen International
Graduate school
Shenzhen, China
yang.cheng@sz.mails.tsinghua.edu.cn

Abstract—Because of excellent power density, good reversibility, and superior stability, supercapacitors have attracted more attention in microelectronic system developments. However, the large-scale preparation of high-performance supercapacitors with low-cost and high mechanical flexibility is still challenging. Herein we report the convenient fabrication of an all-in-one pseudocapacitor by magnetron sputtering and electro-deposition of a MnO₂@Ni cathode and an activated carbon@Ni anode on the two sides of a glass fiber separator. Specifically, the MnO₂ cathode deposited on Ni Nanocone arrays (NNAs) showed good cycle performance (92.2% after 5000 cycles) and excellent capacitance (644 F/g) and. The NNAs@AC (activated carbon) anode deposited on the other side showed a 224 F/g high capacitance and favorable cycle performance (105.9% after 5000 cycles). Benefiting from the special integration method, the porous architecture of the electrodes, and the use of zinc ions as the charge carrier, our all-in-one device achieved favorable mechanical flexibility, high energy density (103.4 Wh/kg at 1.7 kW/kg) with a long cycle (76% after 5000 cycles). Besides, our fabrication approach can be easily extended to the mass production of low-cost devices and provides a new alternative strategy for flexible high-performance energy storage devices.

Keywords—MnO₂; all-in-one; flexible device; Ni nanocone

I. INTRODUCTION

With the increasing demand for flexible electronic devices, there are more market spaces for the corresponding flexible energy storage devices[1-4]. Supercapacitors, with excellent cycle stability, high power density, and other advantages, have been widely involved in a variety of energy storage devices[5-7]. Supercapacitors can already be used in practical where need high power output, but may not be able to reach their maximum storage capacity, which limits their use in energy storage devices[5,8-9]. Thus, a core challenge in supercapacitors' application is how to increase both of their power density and energy density. Developing a way for integration to increase the occupancy of active materials which is a benefit to promote the energy density[2, 10-13]. For example, the direct integration of a carbon-based micro

supercapacitor on a silicon substrate in a wafer-level process was proposed and a high energy density was achieved[14]. Another way to develop it is to improve the current collector. Large surface area and good conductivity of the current collector can also promote the energy density significantly[15-17]. However, the existing technology is still very complex and may encounter difficulties in application. Therefore, developing a mechanically flexible device with high performance, low cost, high electrochemical reversibility, and convenience for industrialization are highly important.

Herein, we reported an all-in-one integration method to integrate the current collector. On this basis, we developed Ni nanocone arrays as the current collector which owns a large specific surface area with good conductivity; and Zn²⁺ ions were used as the conducting ions to reach high energy density for the supercapacitor. At first, magnetron sputtering was used for coated nickel metal on both sides of glass fiber (GF), then we deposited nickel nanocone arrays on the Ni@GF electrochemically. The MnO₂ nanostructure was then deposited on the nickel nanocone arrays to obtain the NNAs@MnO₂ hierarchical porous cathode. Activated carbon was coated similarly on the Ni nanocone arrays to obtain the NNAs@AC anode. The whole process was low-cost and can be extended to roll-to-roll processes easily. At 1 mV/s, the NNAs@MnO₂ presented a 644 F/g excellent specific capacitance, and the NCM@AC showed a 224 F/g excellent capacitance. The NCM@MnO₂ electrode showed good cycle performance with a 92.2% capacitance retention after 5000 cycles, and the NCM@AC electrode showed excellent cycle performance with a 105.9% capacitance remained after 5000 cycles. Our integrated device assembled by NNAs@MnO₂ and NNAs@AC showed high energy density (103.4Wh/kg at 1.7kW/kg) and after 5000 cycles a 76.0% capacitance retention. With multivalent ions, the all-in-one device is promising in future high energy density flexible equipment.

II. EXPERIMENTAL SECTION

A. Preparation of NNAs@GF

The NNAs@GF was prepared by magnetron sputtering and electrochemical deposition. At first, nickel-metal coated on both two sides of the GF by magnetron sputtering and then immersed into the electrochemical deposition solution for NNAs preparation. Using the nickel foil as the counter electrode and using the Ni coated GF as a working electrode. Electrodeposition solution was composed of 0.84 M $\text{NiCl}_2 \cdot 6\text{H}_2\text{O}$, 0.65 M H_3BO_3 , and 1.86 M NH_4Cl . The pH value was adjusted to 4.0 by $\text{NH}_3 \cdot \text{H}_2\text{O}$ and maintained at 60 °C in a water bath. The Ni nanocone coated GF was electrodeposited at a 20 mA/cm² current density for 20 min, 3 times washed by soaking in ultrapure water, then dried the electrode at 60°C overnight.

B. Fabrication of NNAs@MnO₂, NNAs@AC electrode, and the all-in-one device

The NNAs@MnO₂ electrode was prepared by electrodepositing MnO₂ on NNAs coated GF. The deposition process proceeded in 0.1 M $\text{Mn}(\text{Ac})_2$ solution with a 10 mA/cm² current density. Using the NNAs@GF as the working electrode and using Pt foil as the counter electrode. The obtained NNAs@MnO₂ electrode was washed by ultrapure water and dried at 60°C overnight. Polyvinylidene fluoride (PVDF), conductive black, and AC was blended with N-methyl-2-pyrrolidone (NMP) with a 1:1:8 mass ratio, then obtain the paste by magnetic stirring for 6h and then pasted on NNAs coated GF to obtain NNAs@AC. Then we assembled an asymmetrical supercapacitor by preparing both two electrodes on two sides of one GF membrane to form an all-in-one supercapacitor device.

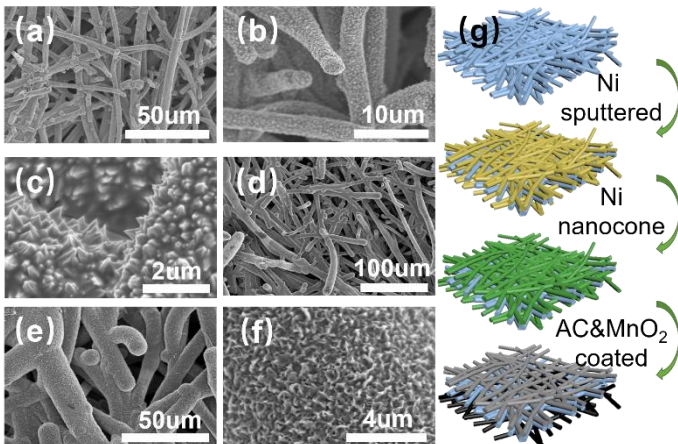


Fig. 1 (a-c) SEM images of NNAs coated glass fibers; (b-f) SEM image of NNAs@MnO₂; (g) Scheme of the fabrication process of the all-in-one device.

C. Materials characterization and electrochemical tests

Using an X-ray diffractometer (XRD, D8 Advance) for collecting the structural information. Scanning electron microscopy (SEM, HITACHI S4800) was used to observe the electrodes' microscopic morphologies. Electrochemical workstation (VMP3, Bio-Logic) was used for testing the electrochemical impedance spectroscopy (EIS), galvanostatic charging-discharging (GCD), and cyclic voltammetry (CV) curves of the electrode and device. Using silver chloride electrode (SCE) and Pt foil as the reference electrode and the counter electrode for three-electrode system testing. The electrolyte was prepared by dissolving 0.1 M MnSO_4 and 0.5 M ZnSO_4 in ultrapure water. The CV's and GCD's potential window of NNAs@MnO₂ electrode was 0 to

0.9 V. The CV's and GCD's potential window of NNAs@AC electrode was -0.8 to 0 V. The CV's and GCD's potential window of the device was 0 to 1.7 V.

III. RESULTS AND DISCUSSION

In figure 1, the SEM image indicates the nickel nanocone arrays and the NNAs@MnO₂ sample. As shown in figure 1, the specific surface area of the current collector increased obviously because of the 3D architecture. Subsequently, MnO₂ was deposited on the nickel nanocone arrays by electrochemical deposition. SEM showed that the manganese dioxide deposited uniformly, which also indicated that the NNAs electrode prepared had a very good electrical conductivity.

In figure 2a, the XRD pattern shows that Ni has high crystallinity, and the pattern can be well-matched with Ni (JCPDS: 04-0850). The XRD pattern in figure 2b shows the presence of MnO₂, indicating that MnO₂ was successfully deposited in the electrochemical deposition process. The two extra peaks can be well-matched with MnO₂ (JCPDS: 30-0820). The lower peak intensity indicates that the crystallinity of manganese dioxide is low, which is consistent with the previous reports[15].

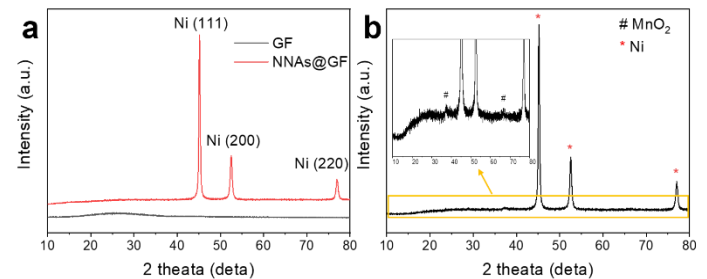


Fig. 2 (a) GF's and NNAs@GF's XRD patterns; (b) XRD pattern of NNAs@MnO₂ electrode

NNAs@MnO₂ electrode was measured in 0.1 M MnSO_4 and 0.5 M ZnSO_4 using a three-electrode system for collecting the electrochemical performance. MnSO_4 can prevent the dissolution of MnO₂ for better cycling performance. The use of mild electrolyte can prevent the device and the electrode material from corrosion, thus improve the cycle performance.

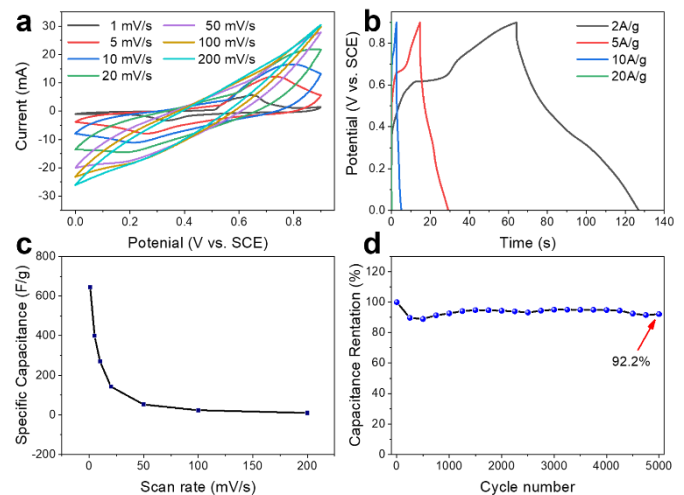


Fig. 3 (a) The CV curves of the NNAs@MnO₂ (1 mg/cm²); (b) The GCD curves (from 2 to 20 A/g) of the NNAs@MnO₂; (c) The NNAs@MnO₂'s specific capacitance at different rates; (d) Capacitance retention of NNAs@MnO₂ at 100 mV/s after 5000cycles.

In figure 3a, when 0 to 0.9 V is selected as the operating voltage window, two obvious redox peaks indicate the pseudocapacitance effect. The platform of GCD curves in figure 3(b) is also helpful for demonstrating this behavior. For the preparation of MnO₂ cathode, after 5 minutes of deposition, the MnO₂ deposited 1 mg/cm² on the electrode. The NCM@MnO₂ electrode shows excellent 644 F/g capacitance and good cycle performance, with capacitance retention 92.2% after 5000 cycles. However, in different scan rates, there is a significant decrease in specific capacitance. Comparing to commonly-used Na⁺ ions as the charge carrier, Zn²⁺ ion has a large mass and two charges, which indicates the capacitance is lower at a high scan rate and higher at a low scan rate.

The NNAs@AC electrode was tested in an aqueous electrolyte (0.5M ZnSO₄ + 0.1M MnSO₄) by a three-electrode system similarly for collecting the electrochemical performance. The NNAs@AC electrode was prepared simply by coating activated carbon on NNAs@Ni@GF. A lower capacitance shows at a high scan rate and a higher capacitance shows at a low scan rate were observed similarly. And the CV curve shows a rectangle shape in figure 4a, which indicates an obvious electric double-layer capacitor (EDLC) capacitance effect. In figure 4b, the GCD curves of the NNAs@AC electrode shows from 2A/g to 10A/g. The GCD curve shows a nonlinear line under a low scan rate. The NNAs@AC shows a 224 F/g excellent capacitance at 1 mV/s, which attributed to a large mass and two charges of Zn²⁺. Similarly, capacity decreases obviously as the scan rate increases (Figure 4c). Cycle performance of the NNAs@AC was measured by the CV test (Fig. 4d), which shows high capacitance retention 105.9% of the electrode after 5000 cycles (100 mV/s). All the results above demonstrate the great electrochemical performance of the NNAs@AC in the zinc ion supercapacitor.

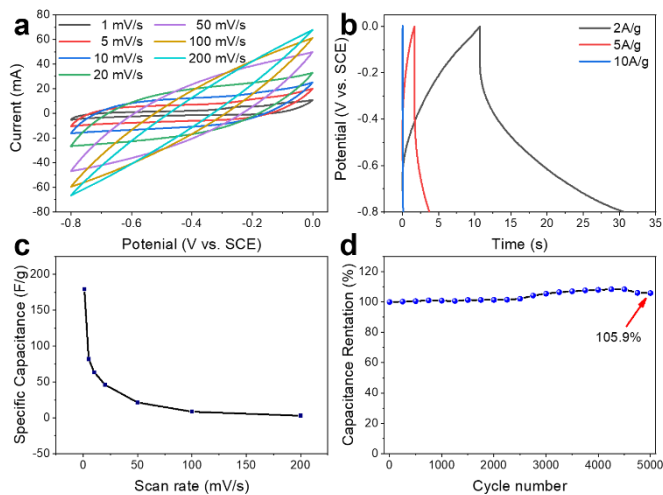


Fig. 4 (a) CV curves of the NNAs@AC; (b) GCD curves (from 2 to 10A/g) of the NNAs@AC; (c) The specific capacitance of NNAs@AC; (d) Cycle performance of NNAs@AC at 100 mV/s after 5000cycles.

To evaluate the feasibility of all-in-one integration at the device level, we further assembled coin cells for testing the electrochemical performance and a flexible sandwich for testing the mechanical property. The electrochemical performance of the device was tested in aqueous 0.5 M ZnSO₄ + 0.1M MnSO₄ electrolyte. In figure 5a, two strong redox peaks appear, which means the pseudocapacitance effect. GCD profiles of the device were shown in different current densities in figure 4b. The device shows a 486 F/g excellent capacitance at 1 mV/s. Based on GCD curves, our supercapacitor exhibited excellent energy density (103.4

Wh/kg at 1.7 kW/kg). The charge transfer resistance (R_{ct}) and calculated internal resistance (R_s) of the device are 0.6Ω and 1.5 Ω, better than some of the MnO₂-based electrodes which have reported before[15].

The capacity decreases as the scan rate increases in figure 4c, which is attributed to the large mass of Zn²⁺ ions. In figure 4d, the performance of the NNAs@AC electrode was collected by the CV test, which indicates that the device remains 76.0% capacity after 5000 cycles at 100 mV/s. And CV curves in figure 5e also shows the stability of the device in a different cycle. All the results above demonstrate the great performance of the Zn ion supercapacitors.

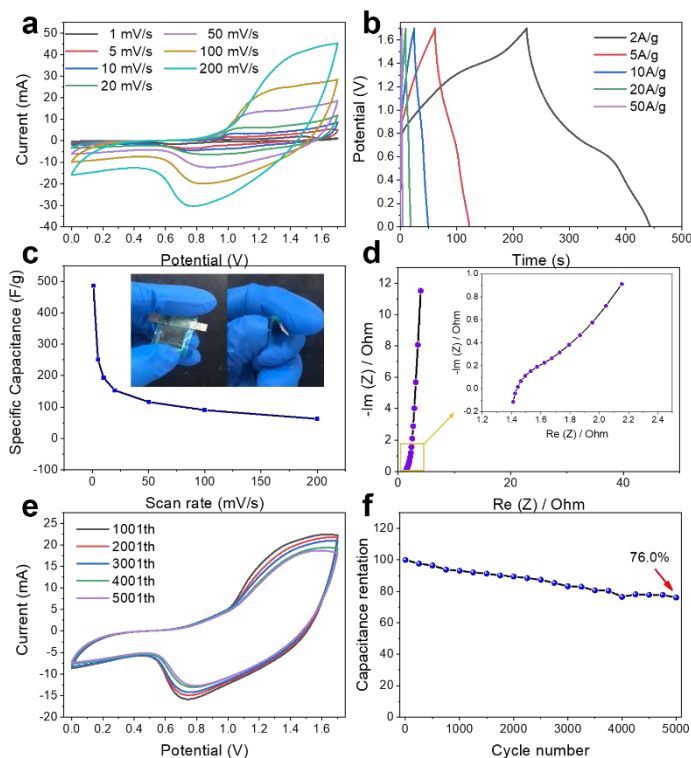


Fig. 5 (a) CV curves of the device; (b) The GCD curves show the performance from 2 to 50 A/g of our device; (c) The specific capacitance of all-in-one device at different scan rate and the insets show a foldable device; (d) Nyquist plots of the device; (e) CV curves in 1001st, 2001st, 3001st, 4001st, and 5001st cycle; (f) Capacitance retention of the all-in-one device at 100 mV/s.

IV. CONCLUSION

We report an all-in-one flexible zinc ion supercapacitor, in which the Ni nanocone arrays are introduced to increase the conductivity and increase the surface area of the NNAs@Ni@GF current collector based on electrodeposition and magnetron sputtering. Benefiting from the all-in-one integration and high conductivity of Ni nanocone arrays, the NNAs@MnO₂ electrode delivered a 644 F/g excellent capacity and superior cycle performance with a 92.2% capacitance retention after 5000 cycles, and the NNAs@AC electrode delivered a 224 F/g excellent capacity and superior cycle performance with a 105.9% capacitance retention after 5000 cycles. The all-in-one devices indicated an ultrahigh energy density of 103.4Wh/kg at 1.7kW/kg and good cycling performance with a 76% capacitance retention after 5000 cycles. Besides, this approach can be conveniently extended to the mass production of low-cost devices and provides a brand new alternative strategy for flexible high-performance energy storage devices in the future.

ACKNOWLEDGEMENT

The authors thank the Local Innovative and Research Teams Project of Guangdong Pearl River Talents Program (2017BT01N111), Shenzhen Geim Graphene Center, Guangdong Province Science and Technology Department (Project No. 2015A030306010), and Shenzhen Government (Project Nos. JCYJ20170412171720306 & JSGG20170414143635496) for financial supports.

REFERENCES

- [1] X. Liu, M. Marlowa, S. Coopera, B. Songb, "Flexible all-fiber electrospun supercapacitor," *Journal of Power Sources*, vol. 384, pp. 264-269, 2018.
- [2] K.-H. Choi, J. Yoo, C. K. Lee, and S.-Y. Lee, "All-inkjet-printed, solid-state flexible supercapacitors on paper," *Energy & Environmental Science*, vol. 9, no. 9, pp. 2812-2821, 2016.
- [3] J. Yan, Z. Fan, T. Wei, W. Qian, M. Zhang, and F. Wei, "Fast and reversible surface redox reaction of graphene-MnO₂ composites as supercapacitor electrodes," *Carbon*, vol. 48, no. 13, pp. 3825-3833, 2010.
- [4] M. Antonietti, X. Chen, R. Yan, and M. Oschatz, "Storing electricity as chemical energy: beyond traditional electrochemistry and double-layer compression," *Energy & Environmental Science*, vol. 11, no. 11, pp. 3069-3074, 2018.
- [5] M. Beidaghi and Y. Gogotsi, "Capacitive energy storage in micro-scale devices: recent advances in design and fabrication of micro-supercapacitors," *Energy & Environmental Science*, vol. 7, no. 3, 2014.
- [6] P. Simon, Y. Gogotsi, and B. Dunn, "Materials science. Where do batteries end and supercapacitors begin?," *Science*, vol. 343, no. 6176, pp. 1210-1, Mar 14, 2014.
- [7] W. Zuo, R. Li, C. Zhou, Y. Li, J. Xia, and J. Liu, "Battery-Supercapacitor Hybrid Devices: Recent Progress and Future Prospects," *Adv Sci (Weinh)*, vol. 4, no. 7, p. 1600539, Jul 2017.
- [8] W. Raza, F. Alib, N. Razac, Y. Luoa, "Recent advancements in supercapacitor technology," *Nano Energy*, vol. 52, pp. 441-473, 2018.
- [9] D. Qi, Y. Liu, Z. Liu, L. Zhang, and X. Chen, "Design of Architectures and Materials in In-Plane Micro-supercapacitors: Current Status and Future Challenges," *Adv Mater*, vol. 29, no. 5, Feb 2017.
- [10] N. A. Kyeremateng, T. Brousse, and D. Pech, "Microsupercapacitors as miniaturized energy-storage components for on-chip electronics," *Nat Nanotechnol*, vol. 12, no. 1, pp. 7-15, Jan 2017.
- [11] F. Wang, X. Wu, X. Yuan, and Z. Liu, "Latest advances in supercapacitors: from new electrode materials to novel device designs," *Chem Soc Rev*, vol. 46, no. 22, pp. 6816-6854, Nov 13 2017.
- [12] Y. Wang, S. Su, L. Cai, B. Qiu, "Monolithic Integration of All-in-One Supercapacitor for 3D Electronics," *Advanced Energy Materials*, vol. 9, no. 15, 2019.
- [13] H. Li, T. Lv, H. Sun, G. Qian, "Ultrastretchable and superior healable supercapacitors based on a double cross-linked hydrogel electrolyte," *Nat Commun*, vol. 10, no. 1, p. 536, Feb 1, 2019.
- [14] H. Durou, D. Pech, D. Colin, P. Simon, P.-L. Taberna, and M. Brunet, "Wafer-level fabrication process for fully encapsulated micro-supercapacitors with high specific energy," *Microsystem Technologies*, vol. 18, no. 4, pp. 467-473, 2012.
- [15] Z. Su, C. Yang, B. Xie, Z. Lin., "Scalable fabrication of MnO₂ nanostructure deposited on free-standing Ni nanocone arrays for ultrathin, flexible, high-performance micro-supercapacitor," *Energy Environ. Sci.*, vol. 7, no. 8, pp. 2652-2659, 2014.
- [16] Z. Hao, L. Xu, Q. Liu, W. Yang, "On-Chip Ni-Zn Microbattery Based on Hierarchical Ordered Porous Ni@Ni(OH)₂ Microelectrode with Ultrafast Ion and Electron Transport Kinetics," *Advanced Functional Materials*, vol. 29, no. 16, 2019.
- [17] Y. Guo, L. Yu, C.-Y. Wang, Z. Lin, and X. W. D. Lou, "Hierarchical Tubular Structures Composed of Mn-based Mixed Metal Oxide Nanoflakes with Enhanced Electrochemical Properties," *Advanced Functional Materials*, vol. 25, no. 32, pp. 5184-5189, 2015.